Scientific Research Publishing

Engineering, 2025, 17(4), 276-288
https://www.scirp.org/journal/eng
ISSN Online: 1947-394X
ISSN Print: 1947-3931

Dynamic Modeling of the Operation of a High Temperature Pressurized Air Production System

Kuiliga Kabore, Souleymane Ouedraogo, Sié Kam, Joseph Dieudonné Bathiebo

Department of Physics, Renewable Thermal Energy Laboratory (L.E.T.RE), Doctoral School of Sciences and Technologies, Joseph KI-ZERBO University, Ouagadougou, Burkina Faso
Email: kabkuiliga@gmail.com

How to cite this paper: Kabore, K., Ouedraogo, S., Kam, S. and Bathiebo, J.D. (2025) Dynamic Modeling of the Operation of a High Temperature Pressurized Air Production System. *Engineering*, **17**, 276-288.
https://doi.org/10.4236/eng.2025.174017

Received: March 7, 2025
Accepted: April 21, 2025
Published: April 24, 2025

Abstract

To install a tower solar power plant, the receiver is a key part for storing heat. There are two categories of receivers: surface receivers and volumetric receivers. To produce pressurized air at very high temperatures, the volumetric receiver is indicated. Thus, it allows the air to be heated up to 1100˚C [1] allowing good efficiency to be achieved. We present here the dynamic modeling of a volumetric solar receiver with pressurized air. The absorber used is designed with ceramic material (terracotta) and a parallelepiped shape called a honeycomb absorber. In our case, the circular cells have a diameter of 3mm and are separated from each other by a distance of 3 mm. The symmetrical character allows us to reduce the calculation domains to an elementary cell representative of their structure. We use the finite element method of the Comsol 5.3a calculation code for the numerical resolution. Our results thus show that with a pressure of 10 bars and an air inlet temperature of 398K˚C for a mass air flow rate of 0.3 kg/s, we obtain an air outlet temperature of around 1000 K, which is sufficient to supply a combustion chamber and drive an alternator.

Keywords

Solar Receiver, Pressurized Air, Honeycomb, Volume Absorber, Comsol

1. Introduction

The economic, social and industrial development of developing countries requires energy management. However, the promotion of renewable energies in general and solar energy in particular, constitutes one of the appropriate solutions for an accelerated development strategy for sustainable development. In the current context of thermodynamic “solar” electricity production, two areas of development

are arousing major interest: parabolic trough power plant technologies and tower power plant technologies. Thermodynamic solar energy conversion systems using tower solar power plants offer promising avenues of research. The solar receiver placed at the top of the tower is a determining element for the efficient operation of a tower solar power plant [1] [2]. However, there are two categories of receivers: surface receivers and volumetric receivers. In addition, the receiver has the role of concentrating solar radiation to transmit heat to a heat transfer fluid, such as air under high pressure, which is the concept of a volumetric receiver. The air pressurized by the compressor is heated in the volumetric receiver to temperatures around 1200 K [3]. The concept of volumetric receivers comes from a temperature limitation of surface receivers. Thus, mastering the operation of volumetric receivers is essential for the installation of tower plants. The objective of this work is the dynamic modeling of the operation of a volume solar receiver with pressurized air for a tower power plant.

2. Materials and Methods

2.1. Description

In order to be able to analyze heat transfers, as well as to better interpret the results, this study is focused on the design of a tower solar power plant based on a Brayton type cycle implemented in a gas turbine (TAG). This technology is known as the HSGT (Hybrid Solar Gas Turbine) plant.

The tower solar power plant is made up of heliostats, a pressurized air volume receiver and a gas turbine with a steam cycle booster which recovers the heat and makes it possible to maintain the operation of the plant in cases of low sunlight (cloudy passage, light veil, etc.) (**Figure 1**).

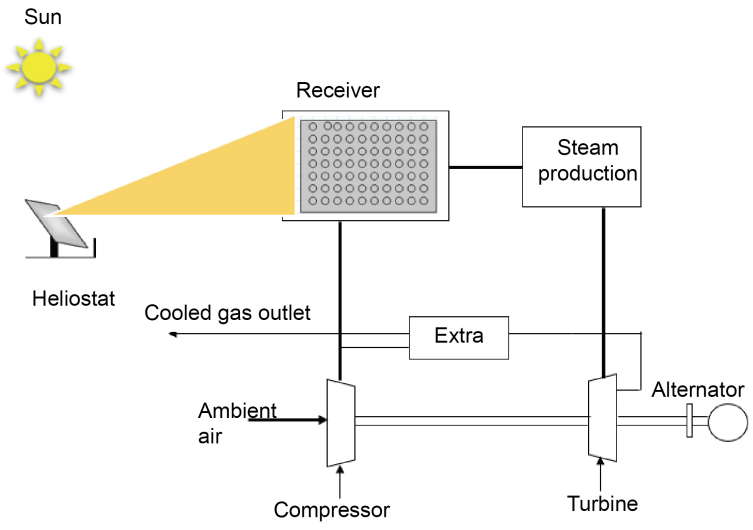

Figure 1. Descriptive diagram of a tower solar power plant: pressurized air receiver.

Air pressurized by compression is used as heat transfer fluid. In the solar re-

ceiver, the air is brought to temperatures varying between 973 and 1200 K, or a little more in the best case, before it is expanded in the turbine, thus producing work to drive an alternator.

2.2. Absorber Technology

The efficiency of the receiver is linked to the quality of the absorber. A material with good heat absorption power would propagate it in large quantities, thus ensuring the permanent operation of the turbine.

The absorber studied in this present work is made of ceramic material. It is a volumetric type receiver characterized by honeycomb-shaped orifices. These orifices are parallel channels with a circular section. All the orifices form a 'honeycomb' of 3 mm in diameter for a straight section. The regular distribution of the orifices makes it possible to reduce the calculation domain on a set of four orifices forming an elementary cell (EC). The entire absorber is made up of 25 × 25 elementary cells, or 625 elementary cells. All of the elementary cells are covered with a layer of vermiculite insulation. Figure 2 shows the diagram of the absorber.

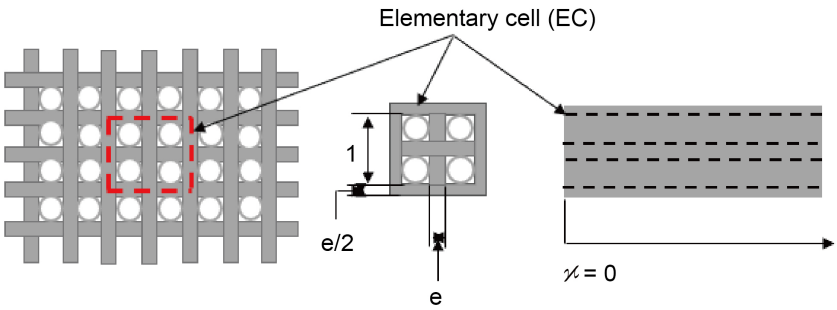

Figure 2. Absorber diagram.

In Figure 3, the flow of the hot fluid is in the direction of *x*.

e: represent the distance between two orifices.

To avoid thermal losses, in our modeling we cover the four faces of an elementary cell with 5 mm of vermiculite.

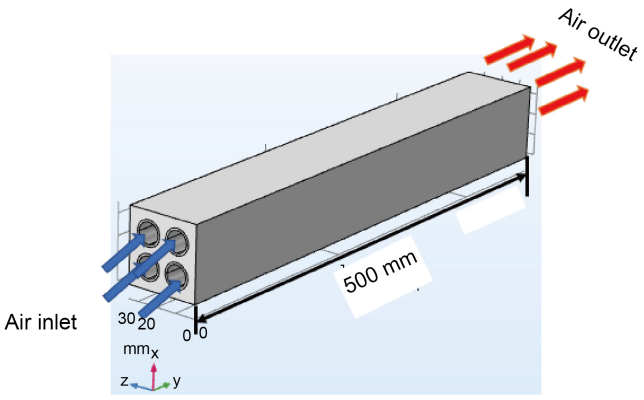

(a)

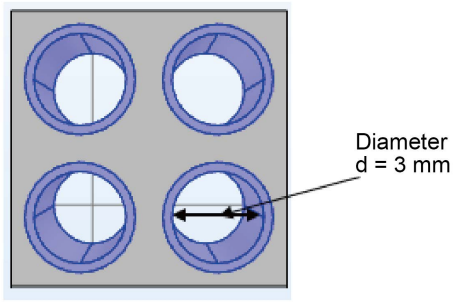

(b)

Figure 3. Diagram of an elementary cell (EC); (a) perspective and (b) front view.

The flow of hot fluid takes place along the *x*-axis. The parameters of the elementary cell used as reference are given by:

- The length $L = 500$ mm along the x axis
- Distance between holes $\mathscr{e} = 3$ mm
- Diameter of holes $d = 3$ mm

2.2.1. Simple Absorber Model

The physical parameters characterizing the absorber are those defined by GOMEZ GARCIA Fabrisio Leopoldo in their thesis work [4]. This is the air inlet temperature in the absorber, the outlet temperature of the absorber, and the temperature inside the absorber characterized by a logarithmic average temperature (**Figure 4**).

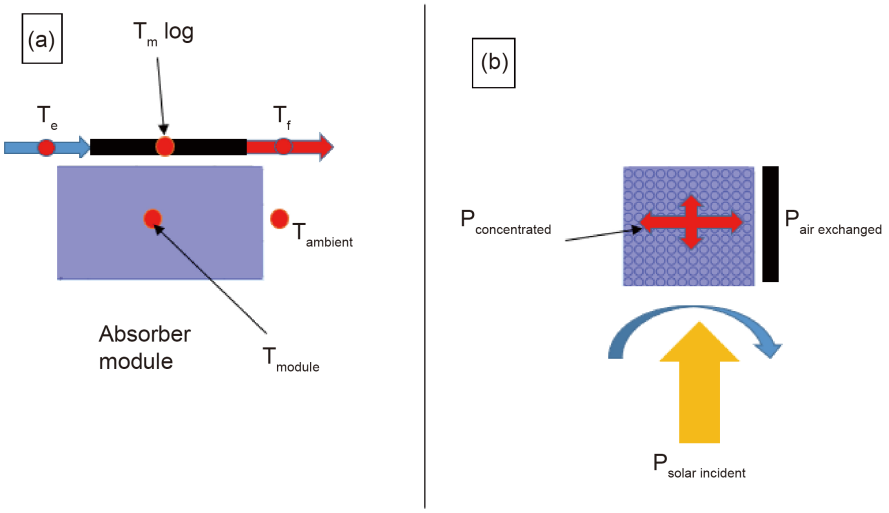

Figure 4. Representation of the physical parameters of the absorber: (a) Temperature and (b) power [5].

To observe a temperature distribution within the exchanger, we use as input parameters, for modeling, a heat flux of 35 kW per m^2. The mass flow rate of air through the orifices of the elementary cell is 0.3 kg/s. The temperature entering the absorber corresponds to that leaving the compressor which is 398 K.

2.2.2. Presentation of the Physical Model in the Comsol Software Interface

Physical description of the system

Our system was studied using the COMSOL Multiphysics software (version 5.3a) by the finite element method (Figure 5).

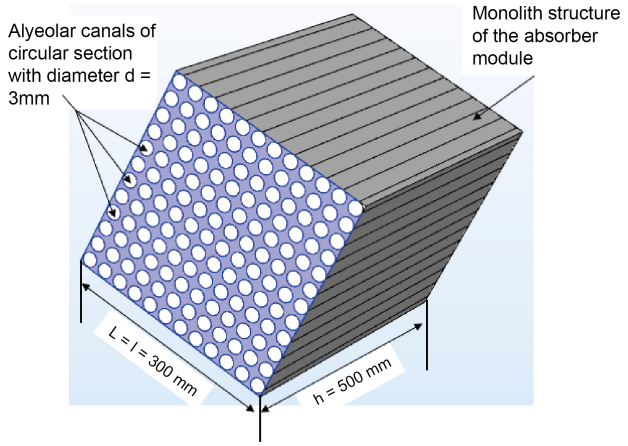

Figure 5. Diagram of the core of the absorber module with COMSOL software.

The performance of such a receiver (with pressurized air) is strongly dependent on the distribution of air at the inlet, and the collection of air at the outlet of the absorber. For good air distribution in the cells and minimal pressure loss, we opt for the use of a conventional distributor associated with a conventional collector. This system makes it possible to standardize the distribution of air in the elementary cells and to maintain the constant air flow and pressure imposed by the compressor (Figure 6).

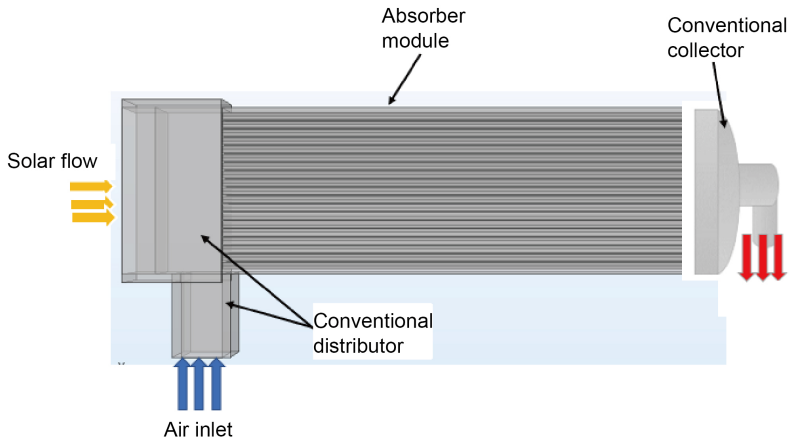

Figure 6. Diagram of the volumetric receiver.

The receiver is supplied with air from the front panel. The compressed air from the compressor is directed to the distributor which supplies the elementary cells of the absorber module. The hot air collected at the outlets of the elementary cells

is routed to the combustion chamber and then to the turbine.

2.3. Definition of Some Concepts

2.3.1. Radiation Penetration Coefficient

The radiation penetration coefficient is a determining parameter for the analysis of the propagation of the luminous flux within the alveolar absorbers. According to the Beer-Lambert law applied in the structures of cellular absorbers, the penetration coefficient a_0 is a function of the axial position x of the elementary cell and the representative dimension of the free section through which the heat transfer fluid flows.

$$a_0 = \frac{\Phi}{\Phi_0 - \Phi_R} = \exp\left(\frac{-x}{l_c \cdot k}\right) \tag{1}$$

x, l_c and k represent the axial position (m), channel size (m) and extension length, respectively.

2.3.2. Solar Power Reflected by Heliostats

The solar power provided by the heliostat field is expressed by the following formula:

$$P_{so} = S_H \times \eta_H \times DNI \tag{2}$$

S_H : Surface area of the heliostats (m²);

η_H : Heliostat field efficiency.

2.3.3. Concentrated Solar Power

It corresponds to the solar power reflected by the heliostats passing through the glass plate at the opening of the receiver cavity and concentrated inside the cavity. In theory it is expressed by:

$$P_{concentrated} = \tau \times a_0 \times P_{so} \tag{3}$$

τ : Transmission coefficient of the window (glass plate);

$P_{concentrated}$: The concentrated solar flux (W).

2.3.4. Solar Power Absorbed by the Module

In theory, the solar power absorbed by the absorber module is the product of the concentrated solar power and the absorbing surface.

$$P_{ab} = \alpha \times P_{concentrated} \tag{4}$$

α : Absorption coefficient of the absorber module.

2.3.5. Thermal Efficiency of the Receiver

The thermal efficiency of the receiver is defined as the ratio between the solar flux transmitted to the air by the absorber and the incident solar flux reflected by the heliostats [6].

$$\eta_{th} = \frac{P_{air}}{P_{so}} \tag{5}$$

$$P_{air} = \dot{m} \cdot C_{pair}\left(T_f - T_e\right) \tag{6}$$

T_f = Outlet temperature;
T_e = Inlet temperature.

2.4. Physical Modeling of the System

From a fundamental physics point of view, we consider here an incompressible, laminar flow in a steady state. Overall, we assume that the flow takes place in a porous medium composed of Si-C and air, with an average porosity equal to 30%.

The conservation equations are then written:

2.4.1. Fluid Mass Conservation Equation

$$\nabla(\rho V) = 0 \tag{7a}$$

In the case of an incompressible fluid the continuity equation is reduced to the form:

$$\frac{\partial u}{\partial x} + \frac{\partial v}{\partial y} + \frac{\partial w}{\partial z} = 0 \tag{7b}$$

2.4.2. Momentum Conservation Equation

According to z it comes:

$$\rho(\boldsymbol{V} \cdot \nabla)\boldsymbol{w} = \nabla(p + \mu\nabla\boldsymbol{w}) \tag{8a}$$

$$\rho\left(u\frac{\partial w}{\partial x} + v\frac{\partial w}{\partial y} + w\frac{\partial w}{\partial z}\right) = -\frac{\partial p}{\partial z} + \mu\left(\frac{\partial^2 w}{\partial x^2} + \frac{\partial^2 w}{\partial y^2} + \frac{\partial^2 w}{\partial z^2}\right) \tag{8b}$$

2.4.3. Energy Conservation Equation in the Fluid

$$\rho C_p \boldsymbol{V} \cdot \nabla T = \nabla(\lambda \nabla T) \tag{9a}$$

$$u\frac{\partial T}{\partial x} + v\frac{\partial T}{\partial y} + w\frac{\partial T}{\partial z} = a\left(\frac{\partial^2 T}{\partial x^2} + \frac{\partial^2 T}{\partial y^2} + \frac{\partial^2 T}{\partial z^2}\right) \tag{9b}$$

With ρ : density; $\boldsymbol{w}$ = air speed; λ = thermal conductivity; μ : dynamic viscosity; a : thermal diffusivity ($m{\cdot}s^{-2}$).

2.4.4. Transfer by Radiation in the Rigid Matrix

In the rigid matrix of the absorber, the heat equation is written taking into account the radiation (absorption and emission).

$$\nabla T_{abs} = q_s \tag{10a}$$

$$q_s = \varepsilon E - \sigma T^4 \tag{10b}$$

2.4.5. Boundary Conditions

- At the inlet, fluid, $z = 0$, power at the inlet = P_w concentrated = 35 kW, T_e = 398 K; P = 10 atm; Flow rate = 0.3 kg/s; P = 10 atm, kept constant.
- At the outlet, we have the jet condition in free atmosphere: $P = P_0$ atmospheric pressure (**Figure 7**).
- On the walls: Losses by convection

$$\phi_{pext} = h_{pext} \cdot S_{ext} \left(T_p - T_{amb} \right) \tag{11}$$

ϕ_{pext} ; S_{ext} ; convective heat loss to the exterior and external surface;
T_p ; T_{amb} ; average wall temperature and ambient temperature.

3. Results and Discussion

3.1. Evolution of the Temperature in the Rigid Matrix

The following hypotheses were considered in this theoretical study:

- The exterior walls are perfectly insulated;
- The distribution of the luminous flux is homogeneous in the entrance plane;
- The thickness of the walls is negligible compared to their length.

Solving the system of Equations (7, 8, 9,) integrating the boundary conditions allows the temperature, speed and pressure fields to be calculated. The latter does not vary practically, since it is practically imposed. Figure 7 reflects the software approach of the temperature evolution as a function of the concentrated flow.

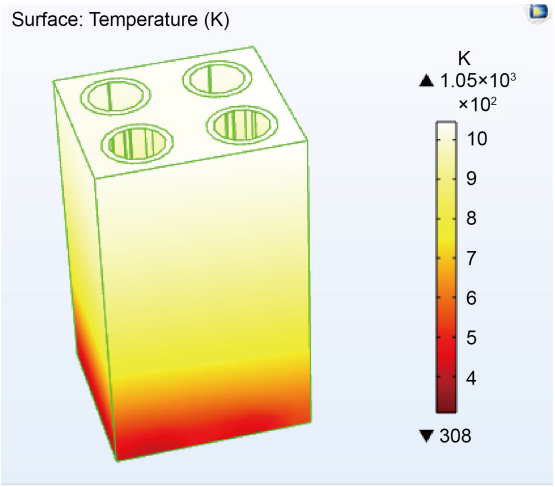

Figure 7. Calculation of the evolution of the temperature in the material, within an elementary cell.

The temperature of the absorber module gradually increases throughout the alveolar channels. Its maximum value recorded at the end of driving and during a day is 1160 K for a concentrated power of 35 kW/m^2 (Figure 8).

3.2. Spatial Evolution of Fluid Speeds

Figure 9 studies a section of the air speed as a function of the height of the elementary cell.

3.3. Evolution of Air Temperature

The air temperature gradually increases along the absorber and reaches its maximum at 900 K with the increasing evolution of the incident solar flux at the same time as that of the solid increases. Figure 10 and Figure 11 show the evolution of the air temperature according to the increasing evolution of the solar flux and for

flow rates varying from 0.1 to 0.5 kg/s.

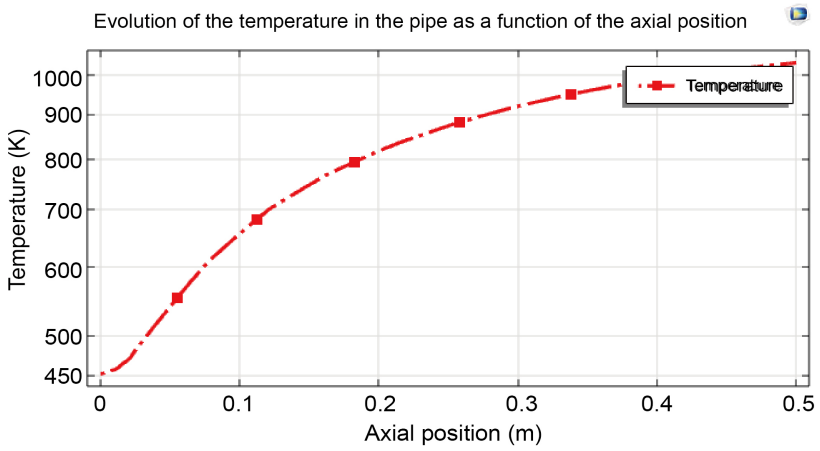

Figure 8. Evolution of the temperature in the pipe as a function of the axial position.

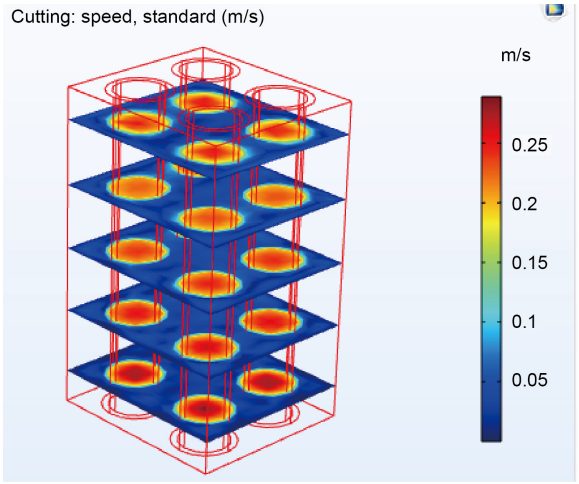

Figure 9. Velocity field.

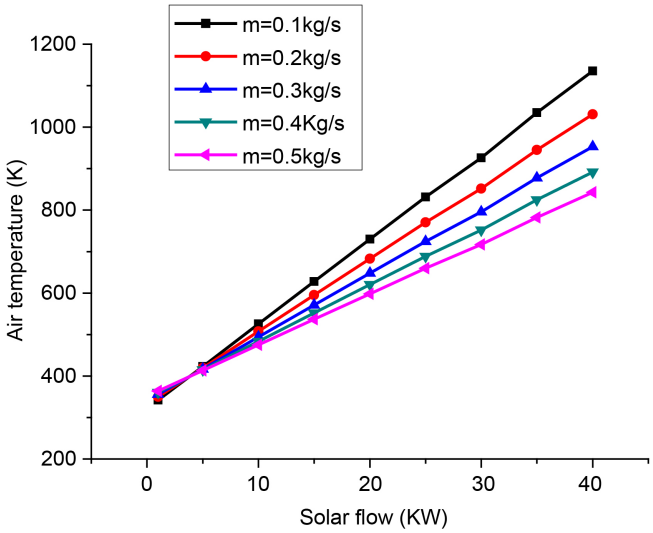

Figure 10. Evolution of air temperature depending on solar flux.

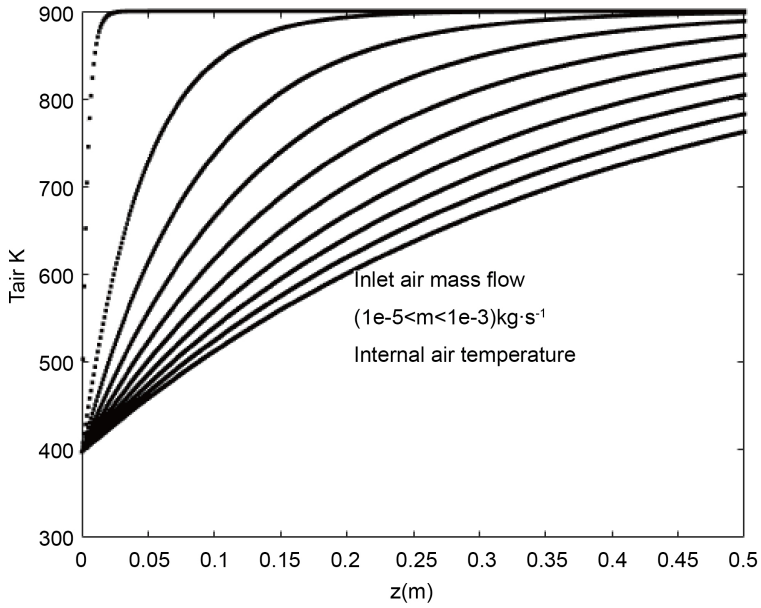

Figure 11. Average air temperatures for different flow rates.

3.4. Thermal Efficiency

From Equation (5), the thermal efficiency of the absorber module characterized as honeycomb highlighted in this present work in steady state is 16%. The constant working pressure (10 bars) and air flow (0.3 kg/s) are imposed by the compressor. The concentrated incident solar power is 35 kW/m^2 with a heliostat surface of 80 m^2.

3.5. Influences of Characteristic Parameters

Several parameters can significantly influence the thermal performance of the absorber module. In this study, in addition to the variation of the incident solar flux, we vary the mass flow rate, the area of the heliostat field and the opening area of the receiver cavity.

3.5.1. Influence of Air Flow

For a constant pressure of 10 bars and an air inlet temperature of 398 K, **Figure 12** studies the influence of the mass air flow on the thermal efficiency of an elementary cell. Indeed, variations in mass flow have a positive influence on thermal efficiency. The higher the mass flow, the greater the thermal efficiency. The flow rate range chosen is between 0.1 kg/s to 0.5 kg/s. The minimum values of thermal efficiency recorded for the different flow ranges are respectively between 1 to 5% and maximum values of 7 to 22%.

3.5.2. Influence of the Heliostat Field Surface

The variations in efficiency were studied numerically for heliostat surfaces of 40 m^2, 60 m^2, 80 m^2 and 100 m^2. Such variations can be obtained for any day of the year using the numerical procedure developed in this research. The elementary

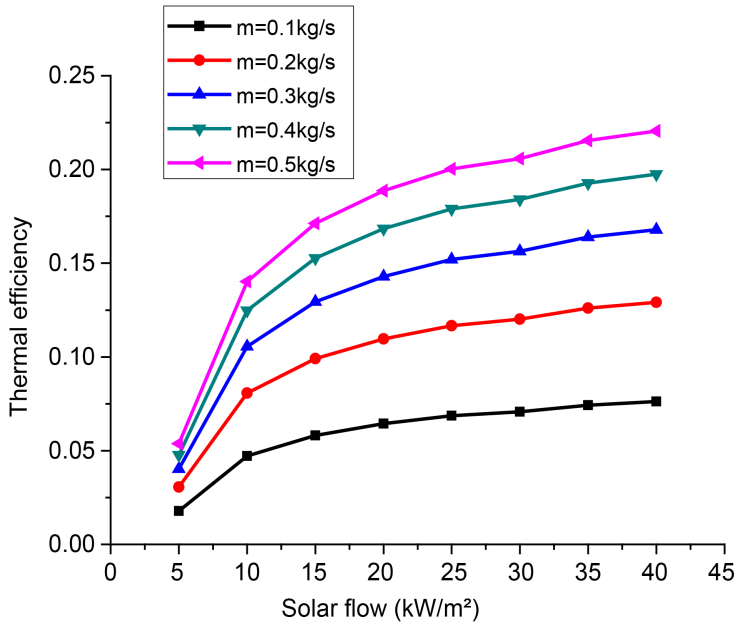

Figure 12. Thermal efficiency as a function of solar flux for a mass flow rate ranging from 0.1 to 0.5 kg/s (Equation (5)).

cell is simulated with a variation of concentrated incident solar power from 1 to 40 kW/m^2 and a constant air flow of 0.3 kg/s. For the same absorber inlet temperature (Ta = 308 K) and air (Te = 398 K), the thermal efficiency evolves in decreasing order (33 to 13%) with an increasing variation in the heliostat surfaces. **Figure 13** shows the evolution of the absorber temperatures as a function of the heliostat surfaces and the concentrated incident solar power.

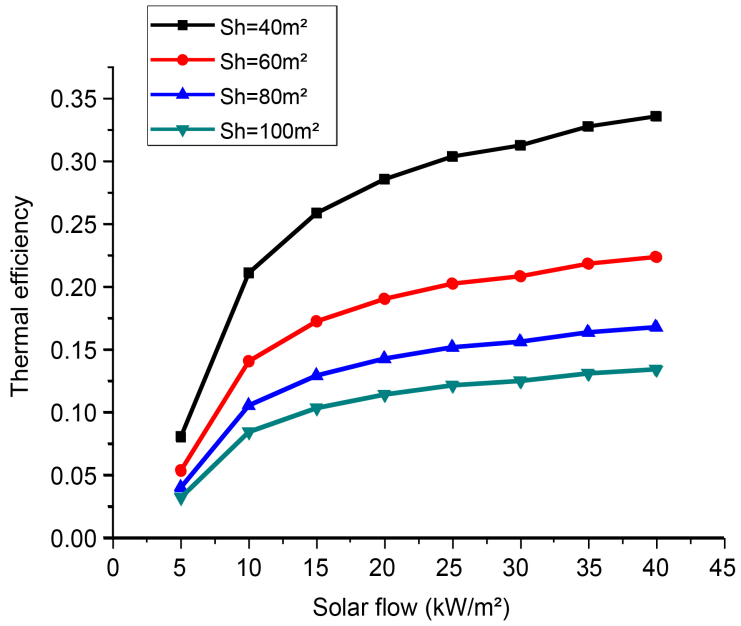

Figure 13. Absorber temperature as a function of solar flux (1 to 40 kW/m^2) for heliostat surfaces of 40 m^2, 60 m^2, 80 m^2 and 100 m^2.

3.5.3. Influence of the Opening Surface

Thermal efficiency is improved by considering an opening surface smaller than the absorber. In fact, an opening surface smaller than the absorber makes it possible to reduce losses by radiation and convection. Figure 14 presents the influence of the opening surface on the thermal efficiency.

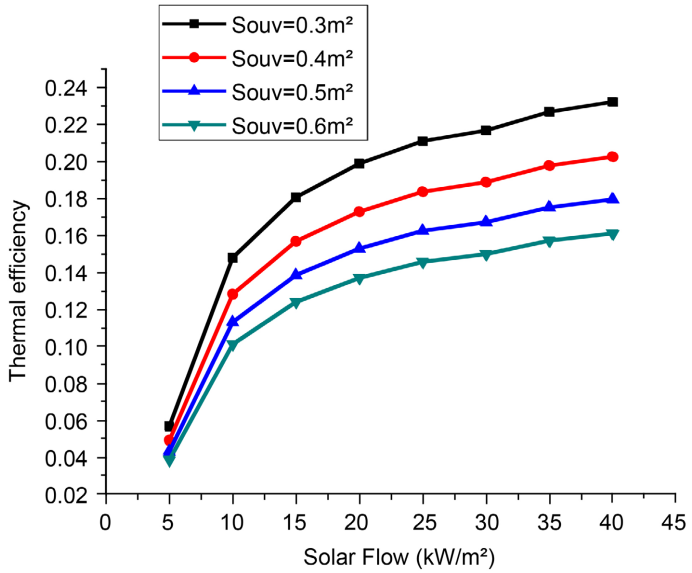

Figure 14. Influence of the opening surface on thermal efficiency (Equation (5)).

The analysis of Figure 13 shows us that the thermal efficiency is improved by considering a smaller opening surface. For a smaller opening surface of around 0.3m², the thermal efficiency is significant, around 23%. And for a large opening surface of around 0.6 m², the thermal efficiency is low, around 16%.

4. Conclusions

We modeled a high temperature pressurized air production system with a ceramic absorber module. For an air temperature of 398 K, an airflow of 0.3 kg/s, a pressure of 10 bar, and a concentrated incident power of 35 kW/m², the thermal efficiency of the receiver is of the order of 16%. Thermal efficiency is improved by considering an opening surface smaller than the absorber. The air outlet temperature gradually increases along the absorber at the same time as that of the solid and this increases according to the value of the solar flux. It reaches its maximum at 900 K depending on the increasing evolution of the incident solar flux.

From this perspective, the model is planned to be developed on an industrial scale for the commissioning of tower solar power plants.

Acknowledgments

The authors gratefully acknowledge the International Science Program (ISP) for supporting BUF01 in Burkina Faso.

Conflicts of Interest

The authors declare no conflicts of interest regarding the publication of this paper.

References

[1] Meriche, I.E. and Beghidja, A. (2012) Modeling and Simulation of a Hybrid Thermal Solar Power Plant with Exhaust Gas Regeneration.

[2] Mohamed, M. and Hamidat, A. (2012) Development of Volumetric Receivers in the Solar Tower.

[3] Sarr, M.P., Thiam, A., Dieng, B. and Ndiaye, F. (2019) Modélisation et simulation d'un système de suivi d'un mini heliostat. *Journal de Physique de la Soaphys*, **1**, C19A9-1-C19A9-4. https://doi.org/10.46411/jpsoaphys.19.01.009

[4] Fabrisio Leopoldo, G.G. (2015) Analysis of the Potential of New Volumetric Absorber Structures for the Receivers of Tower Solar Power Plants. Ph.D. Thesis, University of Perpignan.

[5] Verdier-Gorcias, D. (2016) Thermal Storage for Latent Heat Protection Integrated into a Pressurized Air Solar Receiver. Ph.D. Thesis, University of Perpignan.

[6] Olalde, G. and Peube, J.L. (1982) Experimental Study of a Honeycomb Solar Receiver for Solar Heating of Gases at High Temperatures. https://hal.archives-ouvertes.fr/jpa-00245032

Nomenclature

a_0	Penetration coefficient
DNI	Direct solar radiation, W/m^2;
h_{global}	Global convection coefficient W/m^2·K;
P_{ab}	Solar power absorbed, W;
P_{air}	Thermal power transmitted to the fluid, W;
$P_{concentrated}$	Concentrated solar power, W;
P_{res}	Residual power, W;
P_{So}	Solar power reflected by the heliostats, W;
Φ	The local unabsorbed solar flux, W;
Φ_0	Total incident flow on the front face, W;
Φ_R	Flux reflects, W;
S_{ab}	Surface area of the absorber module, m^2;
T_f	Outlet temperature, K,
T_e	Inlet temperature, K;
T_{abs}	Temperature of the absorber module, K;
η_{th}	Thermal efficiency;